JOURNAL OF MATERIALS SCIENCE 30 (1995) 5043–5048

A mathematical model of the reduction of carbon/alumina powder mixture in a flowing nitrogen stream

H.K. CHEN, C. I. LIN*
Department of Chemical Engineering, National Taiwan Institute of Technology, Taipei, Taiwan 106

A physico-chemical model has been formulated to provide a description of the reduction of carbon/alumina powder mixture in a flowing nitrogen stream. Simultaneous differential equations were derived on the basis of this model. These equations were solved by numerical methods. The chemical reaction rate expression, which was determined in the chemical reaction control region, was used after the model had been employed for interpreting the experimental data. The expressions for effective gas diffusivities, which have been left as a fitting parameter for calculation of theoretical predictions, were determined as

$$D_{e_{Al_2OCO}} = 4.29 \times 10^{-5} \exp(-25971\,J\,mol^{-1}/RT)\ m^2\,s^{-1}$$

$$D_{e_{Al_2OCO_2}} = 2.49 \times 10^{-5} \exp(-31512\,J\,mol^{-1}/RT)\ m^2\,s^{-1}$$

$$D_{e_{Al_2ON_2}} = 3.13 \times 10^{-5} \exp(-29718\,J\,mol^{-1}/RT)\ m^2\,s^{-1}$$

The correlation between the geometrical factor g and half thickness of the sample was determined as $g = 1/(1+64.7L)$, and the correlation between the Sherwood number and Reynolds number was found to be $N_{Sh} = 0.46 N_{Re}^{0.42}$. The reaction occurring between nitrogen, aluminium oxide and carbon was predicted fairly well by this model.

Nomenclature

$C_{Al_2O_3}$, C_C, C_{AlN}	Concentrations of solids Al_2O_3, carbon and AlN, respectively, (kg mol m^{-3})
$D_{e_{Al_2O_3CO}}$, $D_{e_{Al_2O_3CO_2}}$, $D_{e_{Al_2O_3N_2}}$, $D_{e_{COCO_2}}$, $D_{e_{CO_2N_2}}$	Effective normal diffusivities (m^2 s^{-1})
g	Geometric factor (m^{-1})
k_a, k_b, k_c	Reaction rate constants (m^3 s^{-1} kg^{-1} mol^{-1})
K_E	Equilibrium constant
L	Half thickness of solid matrix (m)
N_{Al_2O}, N_{CO}, N_{CO_2}, N_{N_2}	Fluxes of gases Al_2O, CO, CO_2 and N_2, respectively (kg mol s^{-1} m^{-2})
N_{Re}	Reynolds number
N_{Sh}	Sherwood number
N_{Sc}	Schmidt number
P_{Al_2O}, P_{CO}, P_{CO_2}, P_{N_2}	Partial pressures of Al_2O_3, CO, CO_2 and N_2, respectively (atm)
P_t	Total pressure (atm)
R	Gas constant (kJ kg^{-1} mol^{-1} K^{-1})
t	Reaction time (s)
T	Absolute temperature (K)
$X_{Al_2O_3}$, X_C, Y_{AlN}	Conversions of solids Al_2O_3, carbon and yield of solid AlN, respectively
z	Coordinate (m)
ε	Porosity

1. Introduction

The preparation of aluminium nitride, a substrate material used in the electronics industry involves four methods: (1) direct nitridation, (2) chemical vapour deposition, (3) thermal decomposition of diimide, and (4) carbothermic reduction and nitridation. Aluminium nitride produced through direct nitridation contains a large amount of metal ions and impurities. The production cost is high and the raw materials are highly toxic in the methods of chemical vapour deposition and thermal decomposition of diimide. Methods 1–3, therefore, have not yet been made available commercially. The potential for

*Author to whom all correspondence should be addressed.

0022–2461

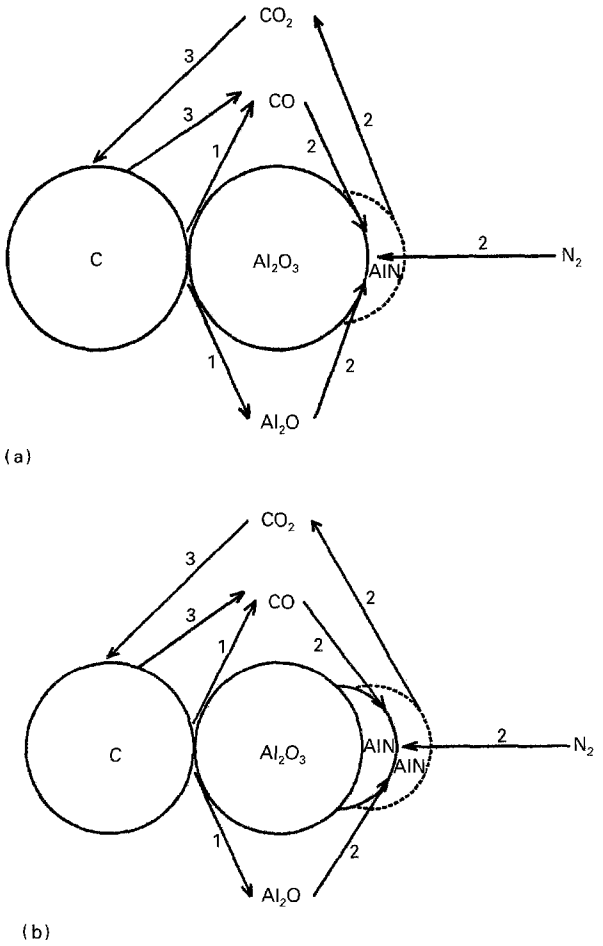

Figure 1 Reaction scheme of the carbothermic nitridation of carbon/alumina powder mixture. (a) Nucleation stage, (b) growth stage.

large-scale production is relatively high for carbothermic reduction.

The reaction between nitrogen and aluminium oxide/carbon powder mixture has been investigated primarily through experiments [1–5]. In previous experiments [5], solid powders of Al_2O_3 and carbon were mixed and poured into a crucible. The crucible was then placed in a tubular furnace and the powders were nitrided by a nitrogen stream. The effects of the following experimental conditions upon the rate of reaction were examined: gas flow rate, reaction temperature, sample height, initial bulk density, weight ratio of Al_2O_3/C, grain size of Al_2O_3 and grain size of carbon. The gas flow rates were usually kept high enough to eliminate the resistance of gas film mass transfer. The reaction rate inferred by the experimental results was increased by increasing the nitrogen flow rate, weight ratio of C/Al_2O_3, or reaction temperature. The rate was also found to be increased by decreasing the sample size, the grain size of carbon or aluminium oxide, or initial bulk density.

The reaction of carbon/alumina powder mixture in a flowing nitrogen stream was thought to take place through the gaseous intermediate Al_2O, in accordance with the following mechanism [5]

$$Al_2O_3(s) + 2C(s) \rightarrow Al_2O(g) + 2CO(g) \quad (1)$$

$$Al_2O(g) + CO(g) + N_2(g) \rightarrow 2AlN(s) + CO_2(g) \quad (2)$$

$$C(s) + CO_2(g) \rightarrow 2CO(g) \quad (3)$$

The reaction scheme is shown in Fig. 1. A solid-solid reaction occurring between Al_2O_3 and carbon produces gaseous Al_2O and CO. Al_2O is adsorbed on to the surface of Al_2O_3 or AlN and reacts with CO and nitrogen in producing AlN and CO_2. The CO_2 gas produced from Reaction 2 simultaneously adsorbed on and reacted with carbon and released CO gas, through Reaction 3.

A physico-chemical model was developed to interpret the experimental data reported by Chen and Lin [5].

2. Development of the model

2.1. Rate expressions

Several elementary steps are involved in Reactions 1–3. The following steps are proposed for this reaction system [5]

$$Al_2O_{3f}(s) + 2C_f(s) \overset{k_1}{\rightarrow} Al_2O(g) + 2CO(g) \quad (4)$$

$$Al_2O(g) + \text{solid surface} \underset{k'_2}{\overset{k_2}{\rightleftharpoons}} [Al_2O]_s \quad (5)$$

$$[Al_2O]_s + CO(g) + N_2(g) \overset{k_3}{\rightarrow} 2AlN(s) + CO_2(g) \quad (6)$$

$$CO_2(g) + C_f(s) \underset{k'_4}{\overset{k_4}{\rightleftharpoons}} CO(g) + [O]_c \quad (7)$$

$$[O]_c \overset{k_5}{\rightarrow} CO(g) \quad (8)$$

Reaction 1 is an elementary reaction. Step 4 is therefore the same as Reaction 1. Reaction 2 contains steps 5–6. A "solid surface" appears in Reaction 5, which includes the solid surfaces of Al_2O_3 and AlN. Al_2O adsorbs on to Al_2O_3 during the nucleation stage, while Al_2O adsorbs both on to Al_2O_3 and AlN during the growth stage. Step 6 represents the reaction between adsorbed Al_2O, CO and N_2. The Boudouard Reaction 3 consists of steps 7 and 8 [6]. Step 7 represents the reaction between CO_2 and carbon, and step 8 the reaction between adsorbed oxygen and carbon.

In the following, $k_1, k_2, k'_2, k_3, k_4, k'_4$ and k_5 will represent the reaction rate constants and C_{AlN}, $C_{Al_2O_3}$, C_c, C_{CO} and C_{CO_2} are the concentrations of AlN, Al_2O_3, C, CO and CO_2, respectively. The following rate expressions can be deduced from the foregoing mechanism [5]

$$\frac{dC_{AlN}}{dt} = k_a C_{Al_2O_3} C_C^2 \Big/ \left(1 + K_E \frac{C_{CO_2}}{C_{CO}}\right)^2 \quad (9)$$

$$\frac{dC_{Al_2O_3}}{dt} = k_b C_{Al_2O_3} C_C^2 \Big/ \left(1 + K_E \frac{C_{CO_2}}{C_{CO}}\right)^2 \quad (10)$$

$$\frac{dC_C}{dt} = k_c C_{Al_2O_3} C_C^2 \Big/ \left(1 + K_E \frac{C_{CO_2}}{C_{CO}}\right)^2 \quad (11)$$

where

$$k_a = 1.6 \times 10^{29} \exp(-565'537/RT)\, d_{Al_2O_3}^{-0.004}\, d_C^{-0.08}\, \rho_0^{-4.9}\ m^3\, s^{-1}\, kg^{-1}\, mol^{-1} \quad (12)$$

$$k_b = -5.6 \times 10^{26} \exp(-465'436/RT)\, d_{Al_2O_3}^{-0.01}\, d_C^{-0.07}\, \rho_0^{-5.0}\ m^3\, s^{-1}\, kg^{-1}\, mol^{-1} \quad (13)$$

$$k_c = -2.7 \times 10^{29} \exp(-640'192/RT)\, d_{Al_2O_3}^{-0.09}\, d_C^{-0.16}\, \rho_0^{-4.3}\ m^3\, s^{-1}\, kg^{-1}\, mol^{-1} \quad (14)$$

$$K_E = 5.83 \times 10^{14} \exp(-427'497/RT) \quad (15)$$

2.2. Dusty gas model

In the dusty gas model, the porous medium is visualized as an array of dust particles held stationary in space. From this viewpoint, the presence of gas–surface interactions is then taken into account by treating the dust particles as giant molecules in terms of the classical kinetic theory of gas [7].

For a binary gas mixture, the diffusive flux, according to the dusty gas model, can be obtained as follows

$$N_j = \frac{-D_{ek_j}}{RT}\nabla P_j - \sum_{k=1}^{n}\frac{D_{eK_j}}{D_{ejk}}(y_k N_j - y_j N_k) - y_j\left(\frac{B_0 P_t}{RT\mu}\right)\nabla P_t \quad (16)$$

2.3. Formulation

Considering a slab-like powder matrix made up uniformly from mixed solid grains consisting of species Al_2O_3 and carbon, which react to form the solid product AlN through the gaseous intermediate Al_2O, according to Equations 1–3 [5], the following assumptions are made.

1. The system is isothermal and isobaric.
2. The structure of the solid matrix does not change during reactions.
3. Pseudo-steady state assumption is applicable to the mass balances of gases.
4. Mass transfer coefficients h_{Al_2O}, h_{CO}, h_{CO_2} and h_{N_2} are equal.
5. The system is in the molecular diffusion region.

The fluxes of components Al_2O, CO, CO_2 and nitrogen derived on the basis of the dusty gas model are employed in the following. The mass balances of gases Al_2O, CO, CO_2 and nitrogen, as well as solids Al_2O_3, carbon and AlN are also made.

Mass balances for components Al_2O, CO, CO_2 and nitrogen lead to Equations 17–24

$$\frac{dP_{Al_2O}}{dZ} = -\left(\frac{RT}{D_{e_{Al_2OCO}}}\right)\left[\left(\frac{P_{CO}}{P_t}\right)N_{Al_2O} - \left(\frac{P_{Al_2O}}{P_t}\right)N_{CO}\right] - \left(\frac{RT}{D_{e_{Al_2OCO_2}}}\right)\left[\left(\frac{P_{CO_2}}{P_t}\right)N_{Al_2O} - \left(\frac{P_{Al_2O}}{P_t}\right)N_{CO_2}\right] - \left(\frac{RT}{D_{e_{Al_2ON_2}}}\right)\left[\left(\frac{P_{N_2}}{P_t}\right)N_{Al_2O} - \left(\frac{P_{Al_2O}}{P_t}\right)N_{N_2}\right] \quad (17)$$

$$\frac{dP_{CO}}{dZ} = -\left(\frac{RT}{D_{e_{COAl_2O}}}\right)\left[\left(\frac{P_{Al_2O}}{P_t}\right)N_{CO} - \left(\frac{P_{CO}}{P_t}\right)N_{Al_2O}\right] - \left(\frac{RT}{D_{e_{COCO_2}}}\right)\left[\left(\frac{P_{CO_2}}{P_t}\right)N_{CO} - \left(\frac{P_{CO}}{P_t}\right)N_{CO_2}\right] - \left(\frac{RT}{D_{e_{CON_2}}}\right)\left[\left(\frac{P_{N_2}}{P_t}\right)N_{CO} - \left(\frac{P_{CO}}{P_t}\right)N_{N_2}\right] \quad (18)$$

$$\frac{dP_{CO_2}}{dZ} = -\left(\frac{RT}{D_{e_{CO_2Al_2O}}}\right)\left[\left(\frac{P_{Al_2O}}{P_t}\right)N_{CO_2} - \left(\frac{P_{CO_2}}{P_t}\right)N_{Al_2O}\right] - \left(\frac{RT}{D_{e_{CO_2CO}}}\right)\left[\left(\frac{P_{CO}}{P_t}\right)N_{CO_2} - \left(\frac{P_{CO_2}}{P_t}\right)N_{CO}\right] - \left(\frac{RT}{D_{e_{CO_2N_2}}}\right)\left[\left(\frac{P_{N_2}}{P_t}\right)N_{CO_2} - \left(\frac{P_{CO_2}}{P_t}\right)N_{N_2}\right] \quad (19)$$

$$P_{N_2} = P_t - P_{Al_2O} - P_{CO} - P_{CO_2} \quad (20)$$

$$\frac{dN_{Al_2O}}{dZ} = (0.5k_a - k_b)C_{Al_2O_3}C_C^2\Big/\left(1 + K_E\frac{C_{CO_2}}{C_{CO}}\right)^2 \quad (21)$$

$$\frac{dN_{CO}}{dZ} = (2k_c - 2k_b - 0.5k_a) \times C_{Al_2O_3}C_C^2\Big/\left(1 + K_E\frac{C_{CO_2}}{C_{CO}}\right)^2 \quad (22)$$

$$\frac{dN_{CO_2}}{dZ} = (0.5k_a - k_c + 2k_b) \times C_{Al_2O_3}C_C^2\Big/\left(1 + K_E\frac{C_{CO_2}}{C_{CO}}\right)^2 \quad (23)$$

$$\frac{dN_{N_2}}{dZ} = -0.5k_a C_{Al_2O_3}C_C^2\Big/\left(1 + K_E\frac{C_{CO_2}}{C_{CO}}\right)^2 \quad (24)$$

The reaction rate expressions of Equations 21–24 have been proposed by Chen and Lin [5]. The definitions of all of these symbols can be found in the Nomenclature.

The conservation of the reactant Al_2O_3 may be written as

$$\frac{\partial C_{Al_2O_3}}{\partial t} = k_b C_{Al_2O_3}C_C^2\Big/\left(1 + K_E\frac{C_{CO_2}}{C_{CO}}\right)^2 \quad (25)$$

For components carbon and AlN the expressions are

$$C_C = \frac{k_c}{k_b}(C_{Al_2O_3} - C_{Al_2O_30}) + C_{CO} \quad (26)$$

$$C_{AlN} = \frac{k_a}{k_b}(C_{Al_2O_3} - C_{Al_2O_30}) \quad (27)$$

The initial concentration of Al_2O_3 is $C_{Al_2O_30}$.

$$C_{Al_2O_3} = C_{Al_2O_30} \qquad \text{at } t = 0 \quad (28)$$

The concentration profiles of gases Al_2O, CO and CO_2 at $t = 0$ are normally unmeasureable. These profiles are typically assumed to be describable by Equations 17–24, into which $C_{Al_2O_3} = C_{Al_2O_30}$ and $C_C = C_{Co}$ are substituted, along with the boundary conditions described below.

There is no diffusion of gases through the bottom of the crucible, hence, the boundary conditions can be written as

$$N_{Al_2O} = N_{CO} = N_{CO_2} = N_{N_2} = 0 \qquad \text{at } z = 0 \quad (29)$$

On the surface of the solid matrix, the flux of mass transfer through the boundary layer equals the diffusive flux in the solid matrix. Therefore, the boundary

conditions on the surface of the solid matrix are

$$N_{Al_2O} = h(P_{Al_2O} - P_{Al_2Ob}) \quad (30a)$$

$$N_{CO} = h(P_{CO} - P_{COb}) \quad (30b)$$

$$N_{CO_2} = h(P_{CO_2} - P_{CO_2b}) \quad (30c)$$

and

$$N_{N_2} = h(P_{N_2} - P_{N_2b}) \qquad \text{at } z = L \quad (30d)$$

If the resistance of mass transfer in the gas film is neglected, the partial pressures of the component gases are equal to those in the bulk gas. The boundary conditions of Equations 30 can be replaced by

$$P_{Al_2O} = P_{Al_2Ob} \quad (31a)$$

$$P_{CO} = P_{COb} \quad (31b)$$

and

$$P_{CO_2} = P_{CO_2b} \qquad \text{at } z = L \quad (31c)$$

Equations 17–31 represent the complete statement of the present problem.

The effective diffusivity in the above equations is a function of porosity and the relation between them is taken to be [8]

$$D_{e_{ij}} = \varepsilon^2 D_{ij} \quad (32)$$

where D_{ij} is the molecular diffusivity.

The extents of the reactions can finally be calculated according to the expressions

$$X_{Al_2O_3} = \frac{1}{L}\int_0^L \left(1 - \frac{C_{Al_2O_3}}{C_{Al_2O_30}}\right) dZ \quad (33)$$

and

$$Y_{AlN} = \frac{1}{L}\int_0^L \left(\frac{C_{AlN}}{C_{AlN0}}\right) dZ \quad (34)$$

3. Solution method

The governing equations, Equations 17–31 are partial differential equations with dependent variables of $P_A(z, t)$, $P_B(z, t)$, $P_C(z, t)$, $N_A(z, t)$, $N_B(z, t)$, $N_C(z, t)$, $N_D(z, t)$, $C_E(z, t)$, $C_F(z, t)$ and $C_G(z, t)$. However, this distributed parameter system can be categorized into boundary value problems, Equations 17–24, and initial value problems, Equations 25–27. The boundary value problems were solved by the BVPMS subprogram of the shooting method [9] and the initial value problems by the RKF45 subprogram [10].

At $t = 0$, $C_{Al_2O_3} = C_{Al_2O_3o}$ and $C_C = C_{Co}$ were substituted into Equations 17–24 to obtain concentration profiles of A, B and C. They were then substituted into Equations 25–27 so as to obtain the values of $C_{Al_2O_3}$, C_C and C_{AlN} at the next time step, $t = \Delta t$. $C_{Al_2O_3}$, C_C and C_{AlN} obtained were then substituted into Equations 17–24 to find P_{Al_2O}, P_{CO} and P_{CO_2} at $t = \Delta t$. The solution was found to be accurate if

$$\left|\frac{\text{solution}|_{\textit{present}\text{ step size}} - \text{solution}|_{\textit{half}\text{ step size}}}{\text{solution}|_{\text{half step size}}}\right| < 1.0 \times 10^{-5} \quad (35)$$

TABLE I The values of variables in carbothermic nitridation experiment

Variable	Value
C/Al_2O_3 weight ratio	17, 8.5, 5.7, 4.25, 2.81
Carbon grain size (10^{-6} m)	0.2, 3.9, 41.4, 68.7, 115.1
Alumina grain size (10^{-6} m)	0.2, 3.9, 41.4, 68.7, 115.1
Sample height (10^{-3} m)	0.5, 1, 2, 4, 8, 13
Initial bulk density (kg m^{-3})	280, 390, 540
Reaction temperature (K)	1623, 1648, 1698, 1748, 1800, 1825
Gaseous flowrate of N_2 (10^5 m^3 s^{-1})	0.9167, 1.25, 1.625, 1.833, 2.1, 2.267, 2.6
CO/N_2 mole ratio	0, 0.001, 0.003, 0.006, 0.01
Porosity	0.51

Over the time scale, $\Delta t = 1800$ s, the above criteria are met, and in the z scale, $\Delta z = 4 \times 10^{-4}$ m in the range of $0 < z < 3.2 \times 10^{-3}$, and $\Delta z = 6.67 \times 10^{-5}$ m in the range of $3.2 \times 10^{-3} < z < 4 \times 10^{-3}$. At each time stage the conversion $X_{Al_2O_3}$ and the yield Y_{AlN} were calculated according to Equations 32 and 33. The iteration continued until either $X_{Al_2O_3}$ or X_C reached unity.

There were three series of experimental runs which have been previously reported by Chen *et al.* [11] in which the effects of pore gas diffusion or mass transfer in the gas film could not be neglected. These experimental results will be interpreted in the light of the proposed mathematical model. The values of some physical properties and critical parameters of the experimental runs are listed in Table I. The underlined values are the standard operating variables. That means when the effect of that variable is not studied, its value is held at the underlined value in that series of experiments.

4. Comparison of results

4.1. Effect of reaction temperature

The experimental results of previous reports [9] are replotted in Fig. 2. The theoretical predictions of the present mathematical model, for example solid lines, are also shown in this figure. The agreements between measurements and calculations are observed here to be rather adequate. Effective diffusivities $D_{e_{Al_2OCO_2}}$, $D_{e_{Al_2OCO_2}}$, $D_{e_{Al_2ON_2}}$ have been left as parameters for the sake of preparing the theoretical curves. The correlations between these diffusivities and temperature are given below

$$D_{e_{Al_2OCO}} = 4.29 \times 10^{-5} \exp(-25'971\ \text{J mol}^{-1}/RT)\ \text{m}^2\,\text{s}^{-1} \quad (36)$$

$$D_{e_{Al_2OCO_2}} = 2.49 \times 10^{-5} \exp(-31'512\ \text{J mol}^{-1}/RT)\ \text{m}^2\,\text{s}^{-1} \quad (37)$$

$$D_{e_{Al_2ON_2}} = 3.13 \times 10^{-5} \exp(-29'718\ \text{J mol}^{-1}/RT)\ \text{m}^2\,\text{s}^{-1} \quad (38)$$

The activation energies thus found are 25'971, 31'512, 29 718 J mol^{-1}, respectively. They are in the range of 25'000–42'000 J mol^{-1}, which is widely accepted as being the activation energy of gas diffusivity [12]. The Arrhenius plots of diffusivities are shown in Fig. 3.

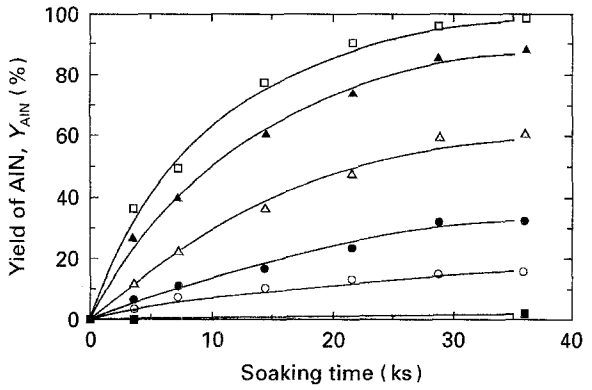

Figure 2 The effect of reaction temperature on the yield of AlN, Y_{AlN} plotted against soaking time, t. (■) 1623 K, (○) 1648 K, (●) 1698 K, (△) 1748 K, (▲) 1800 K, (□) 1825 K.

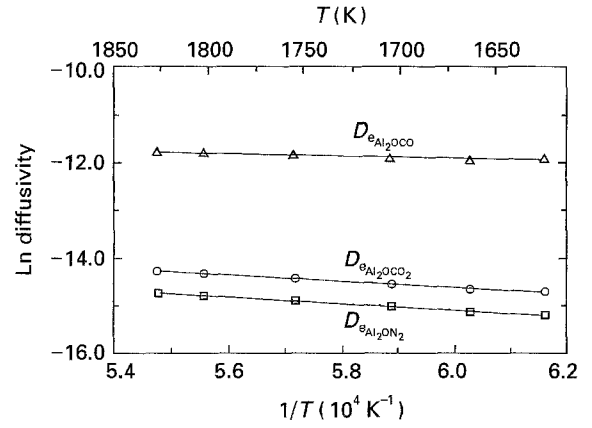

Figure 3 The Arrhenius plots of effective diffusivities.

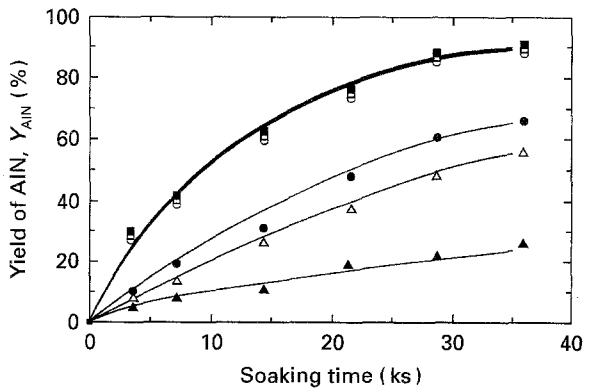

Figure 4 Plot of yield of AlN, Y_{AlN} against soaking time, t and the effect of sample height: (■) 0.0005 m, (□) 0.001 m, (○) 0.002 m, (●) 0.004 m, (△) 0.008 m, (▲) 0.013 m.

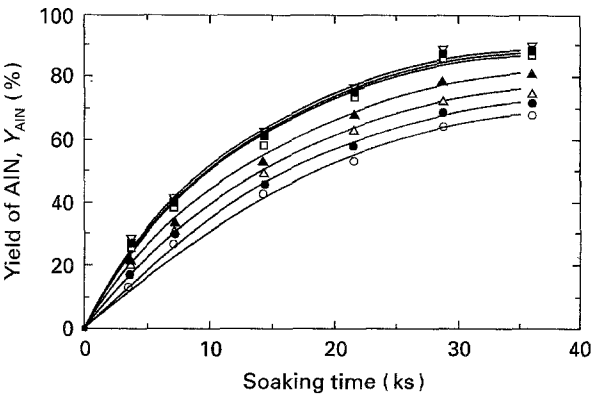

Figure 5 Plot of yield of AlN, Y_{AlN}, against soaking time, t and the effect of gas flow rate (10^5 m^3 s^{-1}): (○) 0.917, (●) 1.250, (△) 1.625, (▲) 1.833, (□) 2.100, (■) 2.267, (▽) 2.600.

4.2. Effect of sample height

The deviation between the prediction of the model and the experimental findings increases once the height of the sample is increased. Two probable reasons are as follows. The temperature in the centre of the solid matrix is lower than that on the surface, owing to the fact that the reaction is endothermic. However, an isothermal assumption has been made during the formulation of the model. The second reason is probably due to the geometry. An infinitely wide plate is assumed to be present in the mathematical model, while the experiments were performed in the crucible which is confined by the wall. As the thickness of the sample is increased, the difference between the model and the experimental conditions is increased.

When the mathematical model is employed to predict the experimental results, the above factors should be taken into account and a geometrical factor, g, is introduced which constructs the effective half thickness of the sample

$$L_{\text{eff}} = L \times g \tag{39}$$

If the half thickness of the sample is replaced by the effective half thickness, the predictions of the model are observed in Fig. 4 to be quite close to those of experimental results. The correlation between geometric factor, g, and half thickness, L, is found to be

$$g = \frac{1}{1 + 64.7L} \tag{40}$$

4.3. Effect of gas flow rate

To prepare the theoretical curves in this case, the mass transfer coefficient, h, was left as a fitting parameter. The calculated curves thus obtained and the experimental data appear in Fig. 5. The calculations and the measurements are found to be fairly good. The obtained mass transfer coefficients, h, were transformed into the Sherwood number and the latter was correlated with the Reynolds number. Their relationship was determined to be

$$N_{\text{Sh}} = 0.46 N_{\text{Re}}^{0.42} \tag{41}$$

in which

$$Sh = \frac{hL}{D_{e_{Al_2OCO}}} \tag{42}$$

$$\text{Re} = \frac{L\rho U_b}{\mu} \tag{43}$$

The crucible holding the solid matrix had the dimensions 0.024 m diameter and 0.002 m thickness. There is no correlated expression between the Sherwood number and the Reynolds number for this geometry. However, a correlation for an infinite flat plate [13] is presented for comparison

$$N_{\text{Sh}} = 0.332 N_{\text{Re}}^{0.5} N_{\text{Sc}}^{0.33} \tag{44}$$

The exponents of the Reynolds number in Equations 41 and 44 are found to be close. This proves that the model is reasonable.

5. Conclusion

A physico-chemical model has been proposed to provide a description of the carbothermic nitridation of carbon/alumina powder mixture. The predictions and measurements were found to be very close. The effective diffusivity was determined to be

$$D_{e_{Al_2OCO}} = 4.29 \times 10^{-5} \exp(-25'971\ \mathrm{J\,mol^{-1}}/RT)\ \mathrm{m^2\,s^{-1}}$$

$$D_{e_{Al_2OCO_2}} = 2.49 \times 10^{-5} \exp(-31'512\ \mathrm{J\,mol^{-1}}/RT)\ \mathrm{m^2\,s^{-1}}$$

$$D_{e_{Al_2ON_2}} = 3.13 \times 10^{-5} \exp(-29'718\ \mathrm{J\,mol^{-1}}/RT)\ \mathrm{m^2\,s^{-1}}$$

and the correlation between geometric factor, g, and the half thickness of the solid sample, L, was found to be

$$g = \frac{1}{1 + 64.7L}$$

The correlation between the Sherwood number and the Reynolds number was

$$N_{Sh} = 0.46\, N_{Re}^{0.42}$$

Acknowledgement

The authors thank the National Science Council of Taiwan for its financial support of this investigation (Grant NSC 82-0402-E-011-114).

References

1. N. KURAMOTO and H. TANIGUCHI, US Pat. 4618592 (1986).
2. H. L. WANG, MS thesis, National Cheng Kung University, Tainan, Taiwan (1988).
3. S. HIRAI, T. MIWA, M. OZAWA and H. G. KATAYAMA, *J. Jpn. Inst. Metals* **53** (1989) 1035.
4. H. INOUE, A. TSUGE and M. KASORI, *J. Mater. Sci.* **25** (1990) 2359.
5. H. K. CHEN and C. I. LIN, *ibid.* **29** (1994) 1352.
6. Y. K. RAO and B. P. JALAN, *Metall. Trans.* **3** (1972) 2465.
7. E. A. MASON, R. B. EVANS and A. P. MALINAUSKAS, *J. Chem. Phys.* **46** (1967) 3199.
8. J. M. SMITH, "Chemical Engineering Kinetics", 3rd Edn (McGraw-Hill, New York, 1981).
9. IMSL "Users Manual, IMSL Math/Library, FORTRAN Subroutines for Mathematical Applications," 11 Edn. (IMSL, Houston, Texas, 1989).
10. G. E.FORSYTHE, M. A. MALCOLM and C. B. MOLAR, "Computer Methods for Mathematical Computations" (Prentice-Hall, Engelwood Cliffs, New Jersey, 1977).
11. H. K. CHEN, C. I. LIN and C. LEE, *J. Am. Ceram. Soc.* **77** (1994) 1753.
12. G. F. FROMENT and K. B. BISCHOFF, "Chemical Reactor Analysis and Design", 2nd Edn. (Wiley, New York, 1976).
13. R. B. BIRD, W. E. STEWART and E. N. LIGHTFOOT, "Transport Phenomena" (Wiley, New York, 1970).
14. H. K. CHEN, PhD thesis, National Taiwan Institute of Technology, Taipei, Taiwan (1994).

Received 22 December 1994
and accepted 2 May 1995